IEEE IAS Annual Meeting
Chicago, Illinois, September 30–October 4, 2001
Paper Number 43-7

Model Reference Current Control of a Unipolar Induction Motor Drive

Brian A. Welchko Thomas A. Lipo

University of Wisconsin – Madison
1415 Engineering Drive
Madison, WI 53706, USA

***Abstract*–A control algorithm to yield the required current shaping control of a three active switch, three-phase unipolar drive system for an induction motor is derived in this paper. The method utilizes terminal voltage control through PWM to properly shape the phase currents. Phase voltages are calculated based on both the fundamental frequency and zero sequence steady-state equivalent circuits of an induction machine to achieve the desired speed and load set point. Since this method relies on characterizing the machine parameters, it does not require feedback of the phase currents, and therefore, drive systems using this method for this topology can eliminate three current sensors over traditional hysteretic current control methods. Both simulation and experimental results are included to verify the proposed terminal voltage control method on this potential low cost variable speed topology for integrated motor-inverter products.**

I. Introduction

For many years, the low voltage variable speed induction motor drive has been centered on the standard 6-switch inverter (B6) topology. While this circuit delivers unparalleled performance, its high cost has been a hindrance for adoption of variable speed drives in the consumer marketplace. Since the cost is a principle driver in the fractional to integral horsepower market, inverter topologies with fewer than six active switches can add significant value to application specific products where the cost of a standard inverter topology cannot be justified [1]. Two such topologies that have received the attention of researchers are the B4 inverter topology with four IGBT switches [2–3], and the delta inverter [4], which uses only three IGBT switches. While the delta inverter is impractical since it requires three isolated dc busses, a new three active switch topology presented in [5] shows promise as a viable candidate for this marketplace since it delivers true variable speed performance with a minimum switch count and uses a low cost diode voltage doubler rectifier front end.

This paper develops a new control algorithm for this topology in which the required current shaping control is achieved via terminal voltage control. This new control method is significant because it requires no current sensors, while the control method demonstrated in [5] required three current sensors as it employed a simple hysteresis current controller. As a result, this unipolar topology using the proposed control method, could achieve significant cost reduction over the conventional B6 or B4 inverters while maintaining all the benefits of variable speed performance.

II. Inverter Operating Principle

The unipolar drive system for a three-phase induction machine is shown in Fig. 1. This topology consists of three phase legs each with an IGBT type switch and diode in a shoot-through free leg structure. The topology is asymmetrical in nature as one of the active switches is connected to the positive dc rail and the other two are connected to the negative dc bus. The dc link of this system is obtained via a voltage doubler type diode rectifier. This link arrangement represents the lowest cost solution to provide the required split capacitor dc bus. This topology requires a non-standard three-phase induction machine. While different, this machine can be obtained simply by externally rewiring the winding connections of a standard induction machine with a dual wound stator winding. Machines that are capable of operating from two different voltages are in this category provided all twelve of the stator leads are available.

The converter operates by controlling the machine phase currents to the shape of the currents shown in Fig. 2. These dc, or unipolar, currents consist of a fundamental component and a zero sequence component made up of a dc offset and triplen harmonics as shown in Fig. 3. The addition of the zero sequence does not produce any useful torque, but makes the currents unidirectional, so the simpler inverter leg structure with only one switch per phase can be used.

One of the phase legs (phase *b* in Fig. 1) must be reversed in this topology in order to create a discharge path for both of the link capacitors. This reverses the direction of current flow in this leg, hence the reversal of the magnetic polarity of that motor phase in order to maintain the same rotational direction of the motor flux. The current in this reversed

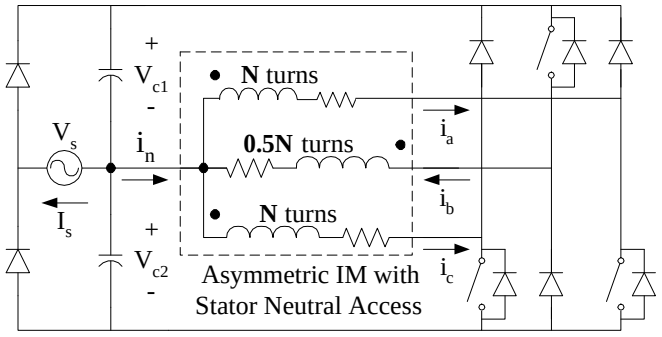

Fig. 1: Unipolar drive topology for an induction machine.

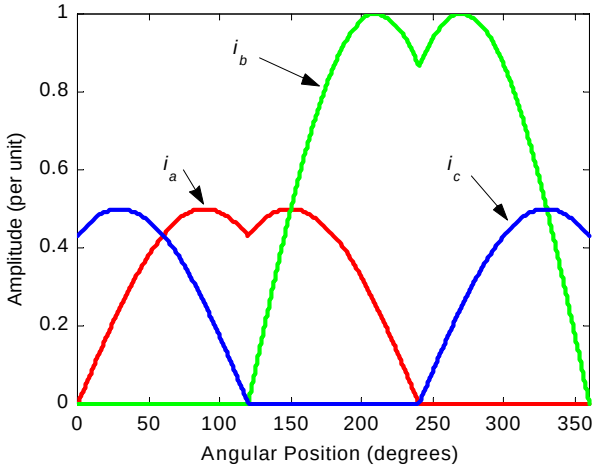

Fig 2: Required shape and magnitude of the motor phase currents for a unipolar induction machine drive.

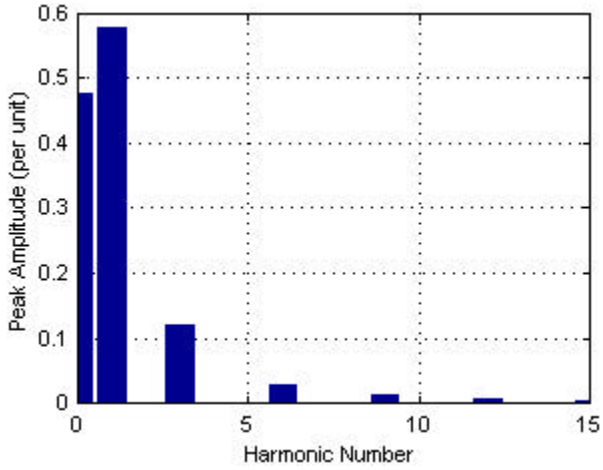

Fig. 3: Phase current harmonic spectrum for current with amplitude 1.

phase must also be double that of the other two phases in order to maintain an even discharge of the link capacitors. To create an equal contribution in amplitude to the motor flux, the number of turns in this phase must be halved to maintain a constant number of ampere-turns in the motor. Essentially this requires that the phase *a* and *c* windings be connected in series while the phase *b* windings are connected in parallel and reversed in magnetic orientation.

III. Terminal Voltage Control

The phase leg structure of this topology is half-controlled. Fig. 4(a) shows the current-voltage plane in which each phase leg can operate while maintaining control. This is in contrast to the fully controlled phase legs of a standard inverter as shown in Fig. 4(b). As a result, through appropriate PWM techniques, this topology can impress any voltage on the phase load, provided the current is greater than zero.

The required voltage to produce the desired phase currents can be obtained from knowledge of the phase current harmonic spectrum and the steady state equivalent circuit

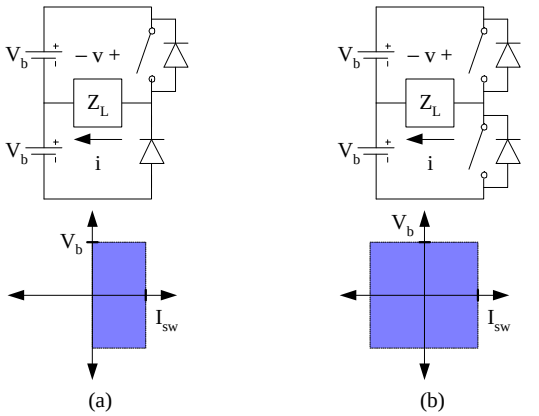

Fig. 4: Current-voltage plane of a half-controlled phase leg (a) and a full controlled phase leg (b).

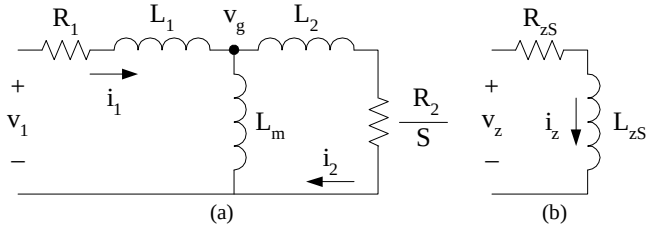

Fig. 5: Induction machine steady-state equivalent circuits: (a) fundamental frequency, (b) zero sequence.

model of the induction machine shown in Fig. 5. Fig. 5(a) shows the fundamental equivalent circuit and 5(b) shows the zero sequence equivalent circuit where L_{zS} is the zero sequence inductance and R_{zS} is the zero sequence resistance. R_{zS} is typically taken to be equal to the stator resistance while L_{zS} is considered to be some percentage (80–95%) of the per phase leakage inductance, L_1, due to saturation effects. [8]. For purposes of this paper, core losses in the machine have been neglected.

Table I gives the phase current definitions in terms of a piecewise combination of sine waves. Table II gives the Fourier harmonic components of the phase *a* current defined in Table I and Fig. 2. Note that in this table, the amplitude of the harmonic components has been normalized to that of the fundamental.

Since the steady state per phase model of the induction machine is a linear time invariant system, the net required applied terminal voltage can be obtained by superimposing the individual harmonic voltages required to produce the desired harmonic current.

TABLE I

PHASE CURRENT DEFINITIONS OVER AN ELECTRICAL CYCLE

Current	Angular Position		
	$0 < \omega t \le 120°$	$120 < \omega t \le 240°$	$240 < \omega t \le 360°$
Phase *a* (i_a)	$I_{max}\sin(\omega t)$	$I_{max}\sin(\omega t - \pi/3)$	0
Phase *b* (i_b)	0	$2I_{max}\sin(\omega t - 2\pi/3)$	$-2I_{max}\sin(\omega t)$
Phase *c* (i_c)	$I_{max}\sin(\omega t + \pi/3)$	0	$I_{max}\sin(\omega t - 4\pi/3)$

Table II

PHASE *a* CURRENT FOURIER HARMONIC COMPONENTS

Harmonic Number (n)	Amplitude (per unit)	Phase Angle Ψ_n (°)
0	0.8270	--
1	1.0000	0
3	0.2068	60
6	0.0473	60
9	0.0207	60
12	0.0116	60
15	0.0074	60
18	0.0051	60

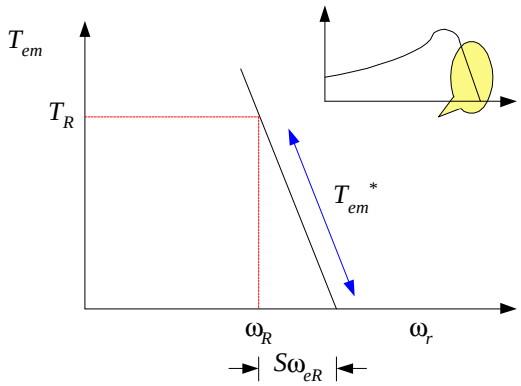

Fig. 6: Steady-state torque and slip frequency relationship.

A. Fundamental Voltage Calculations

For the target application for this drive of fan-type load where the load torque is proportional to the square of the speed, ω_r, the load in the steady state will always be less than or equal to the rated motor torque, T_R. Hence, it can be assumed that the developed motor torque, T_{em}, will vary linearly with slip frequency, $S\omega_e$, as shown in Fig. 6 [6–7].

For a given load, T_{em}^*, the required slip frequency can be found via interpolation as

$$\left(S\omega_e\right)^* = \frac{T_{em}^* S\omega_{eR}}{T_R} \tag{1}$$

The corresponding excitation frequency is then

$$\omega_e^* = \omega_r^* + \left(S\omega_e\right)^* \tag{2}$$

where ω_r^* is the desired rotor speed.

One expression for the developed torque of an induction machine is

$$T_{em} = \frac{\frac{3}{2} i_{2pk}^2 R_2}{S\omega_e} \tag{3}$$

where the subscript *pk* indicates a peak, as opposed to rms, quantity. For the given load, (3) can be solved for the required rotor current as

$$\boldsymbol{i}_{\boldsymbol{2pk}}^* = \sqrt{\frac{2}{3}\left(S\omega_e\right)^* T_{em}^* \frac{1}{R_2}} \tag{4}$$

The required air-gap voltage is then calculated as

$$\mathbf{v}_{\boldsymbol{g\text{-}pk}}^* = \left(\frac{R_2}{S^*} + \mathrm{j}\omega_e^* L_2\right)\boldsymbol{i}_{\boldsymbol{2pk}}^* \tag{5}$$

where boldface font indicates that the quantity contains both magnitude and phase information. Using (4) and (5) along with the fundamental frequency equivalent circuit, the fundamental frequency stator current is

$$\boldsymbol{i}_{\boldsymbol{1pk}}^* = \boldsymbol{i}_{\boldsymbol{2pk}}^* + \frac{\mathbf{v}_{\boldsymbol{g\text{-}pk}}^*}{\mathrm{j}\omega_e^* L_m} \tag{6}$$

Equations (5) and (6) can then be used to give the fundamental frequency phase voltage. This is

$$\boldsymbol{v}_{\boldsymbol{1pk}}^* = \left(R_1 + \mathrm{j}\omega_e^* L_1\right)\boldsymbol{i}_{\boldsymbol{1pk}}^* + \mathbf{v}_{\boldsymbol{g\text{-}pk}}^* \tag{7}$$

Equation (7) gives the fundamental frequency phase voltage required to produce the desired load torque and speed.

B. Zero Sequence Voltage Calculations

Once the amplitude and phase of the torque producing fundamental is solved using the techniques of the preceding section, the zero sequence currents can be found from Table II as they are algebraically related to the fundamental from the Fourier analysis of the desired wave shape. The zero sequence voltage to produce the zero sequence currents can be calculated from the circuit of Fig. 5(b) as

$$\boldsymbol{v}_{\boldsymbol{z\text{-}pk}}^* = \sum_{n=0,3,6,\ldots}^{\infty}\left(R_{zS} + \mathrm{j}\omega_e^* n L_{zS}\right)\boldsymbol{i}_{\boldsymbol{z(n)\text{-}pk}}^* \tag{8}$$

where n represents the harmonic number of the zero sequence current. The 18th harmonic amplitude is only 0.5% of the fundamental, so, in practice, little benefit would result from including more harmonics in the zero sequence voltage calculation. When using (8), it is important to account for the phase displacement of the harmonics to the fundamental (60°) as shown in Table II in addition to the calculated fundamental phase angle in (6).

The net required applied phase voltage to produce the desired phase current amplitude and shape is obtained by

superposition of the fundamental voltage (7) and the harmonic voltage (8) as

$$v_{ph} = v^*_{1pk} + v^*_{z\text{-}pk} . \quad (9)$$

Equation (9) gives the required applied phase voltage for the proposed control algorithm. However it does not account for the asymmetry of the induction motor required for this topology. As a result, reversal of one phase polarity and change in amplitude for that phase must be accounted for when (9) is implemented. For example, if (9) was calculated using motor parameters of the high voltage phases (*a* and *c*), the phase *b* voltage must be reversed in polarity and halved in magnitude to account for the connection of the two phase *b* windings in parallel.

IV. Simulation Results

To verify the proposed algorithm a typical fan load was simulated using SIMULINK®, with data post-processing in MATLAB® for a 1 hp induction motor driven by an ideal unipolar inverter topology. Parameters for the motor used for the simulation are given in the Appendix.

Fig. 7 shows the control system block diagram that was used for the simulation. Since the proposed control algorithm was based on the steady state equivalent circuit model of an induction machine, speed changes should be implemented slowly so that the machine is in quasi-electrical steady state and the model is valid. For the target air moving application, this poor transient performance is not detrimental since the system will change speeds infrequently and a slow response will hardly be noticed. For a smooth transition, both jerk and acceleration limits were imposed on the system. Since the phase leg structure of the unipolar inverter is only capable of controlling a positive current, an additional dc offset is added during speed transients so that even with parameter errors, the motor will be able to draw the required fundamental current to accelerate the load. Once steady state is reached, the dc offset is set back to that calculated in Section III. Using this minimum dc offset will allow the topology to operate at its maximum efficiency.

Controlling the acceleration of the system has an additional benefit; it provides a simple means of controlling the ratio of the peak transient current levels to that of steady state operation. As a result, a better silicon utilization ratio might be feasible when compared to a more traditional V/f control.

A simple speed estimator using the mechanical equivalent circuit and the commanded torque (low pass filtered) is used to provide a feedback signal to the PI type speed controller since the actual motor speed is unavailable for use in this system.

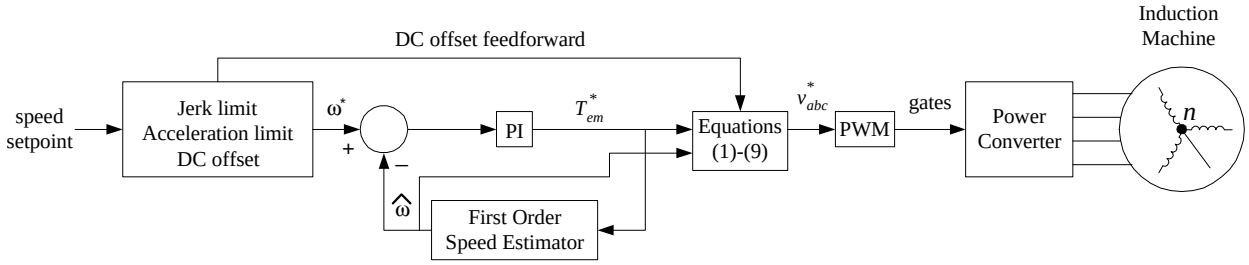

Fig. 7: Control system block diagram.

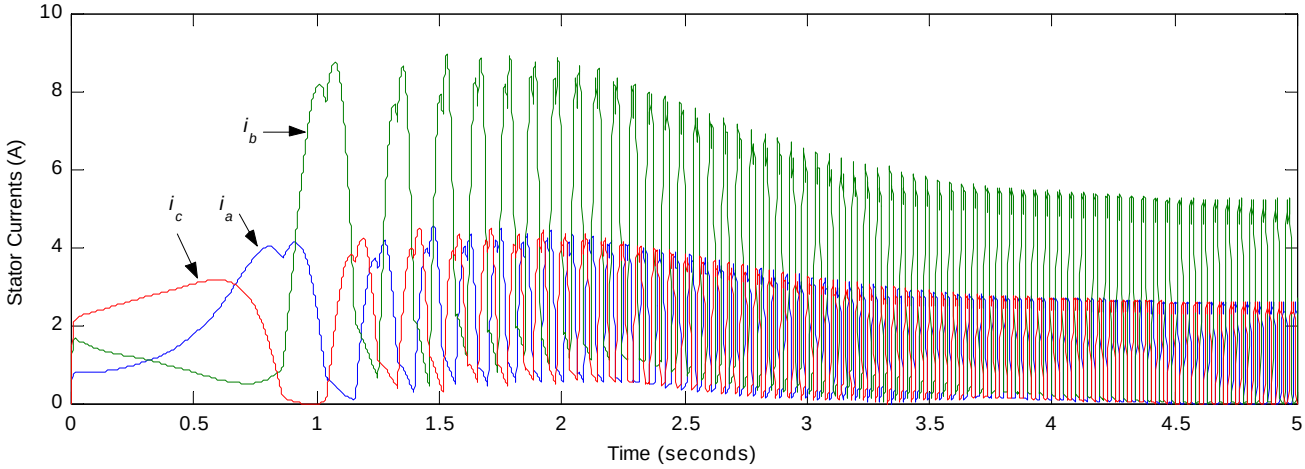

Fig. 8: Phase currents obtained using the proposed voltage control algorithm during acceleration from 0 to 1200 rpm for a fan load. Current polarities as defined in Fig. 1.

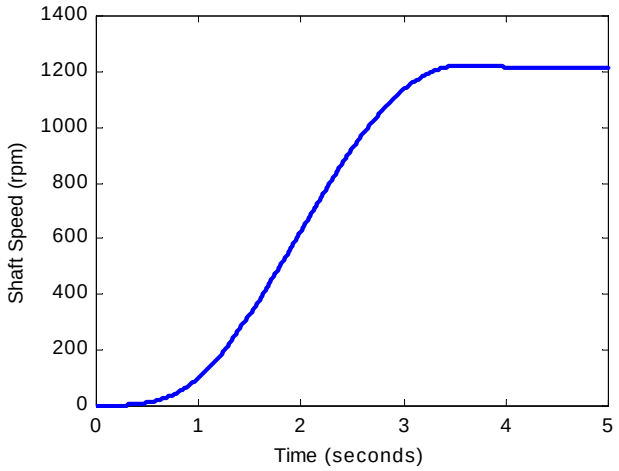

Fig. 9: Simulated motor speed showing strartup.

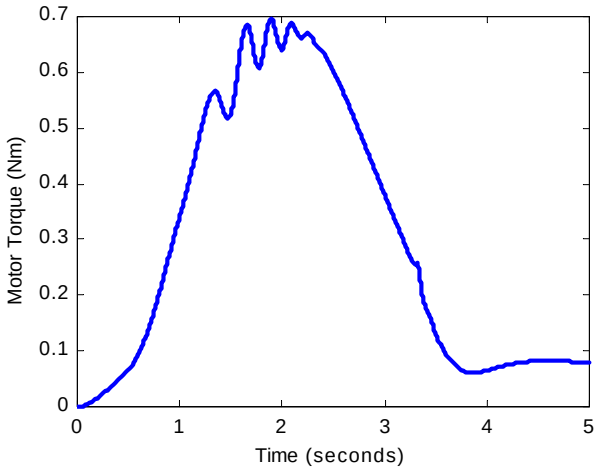

Fig. 10: Simulated motor torque showing startup.

The system was simulated for a speed profile from 0 to 1200rpm for a fan load. Results of this simulation are shown in Figs. 8–11. Figure 8 shows the motor phase currents during acceleration. These currents show evidence of the additional dc offset during the speed transient as the currents are always above zero during a portion of the acceleration. Wave shape agreement during the transient shows some distortion due to errors in the feedback signal (estimate) and the steady state nature of the algorithm.

Figure 9 shows the shaft speed of the motor. The jerk limit is evident during the first 1.5 seconds at which point the control system is commanding a constant acceleration. The reversal of this takes place as the system slows into constant speed mode at 1200rpm. Fig. 10 gives the motor torque for this simulated profile.

Figure 11 shows an expanded view of the motor phase currents once the system has reached steady state. The currents show excellent agreement in wave shape to the theoretical ideal of Fig. 2.

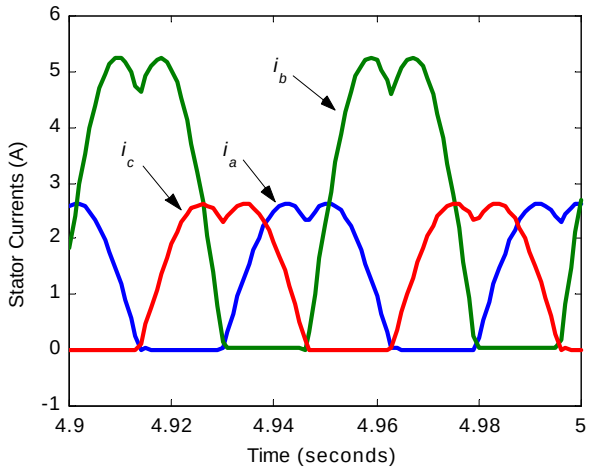

Fig. 11: Expanded view of the steady state phase currents.

V. Experimental Results

The proposed control algorithm was also implemented as a laboratory prototype to verify the simulated results. A Motorola 68805EVM DSP control board was used to control the system with a 10kHz switching frequency.

Implementation of the control algorithm presented in this paper requires several practical considerations for any non-ideal, real world system. The induction machine fundamental equivalent circuit has a speed voltage term associated with it and this back emf of the machine increases with speed. The zero sequence circuit has no speed voltage associated with it. Hence, the zero sequence voltage necessary to induce the desired currents becomes a small percentage when compared to the fundamental voltage as the speed increases. As a result, this algorithm will be more robust in machines with large zero sequence reactances. Also, as the phase *b* voltage of the machine is half that of phases *a* and *c*, phase *b* will be more susceptible to non-linearities in the inverter resulting from voltage drops in the devices. These device drops (assumed constant) were measured in the experimental setup and compensated for in the commanded voltage profile.

The machine available for testing purposes has a very small leakage reactance component, about 5%. This proved to be insufficient in order to control the phase currents with the proposed algorithm. As a result, it was necessary to increase the zero sequence reactance of the test machine. This was accomplished by placing a 5.5mH inductor in the neutral leg of the machine.

Figures 12–13 show the measured phase currents and neutral current for the test machine operating in an unloaded condition. The polarities of the currents in these figures correspond to polarities as in indicated in Fig. 1. The commanded machine speed was 1200 rpm and the actual resulting speed was 1198 rpm. This speed was chosen for target air handling application and not as an effort to de-rate the higher speed machine which otherwise met the qualifications needed for this topology.

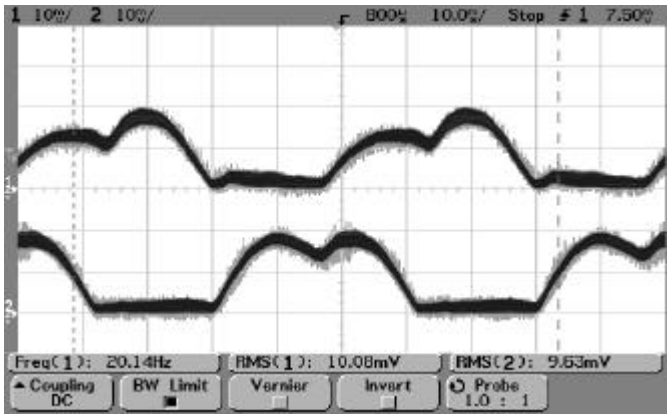

Fig. 12: No-load experimental phase currents. 2A/div. Top trace: Ch. 1, Phase *a*. Bottom trace: Ch. 2, Phase *c*.

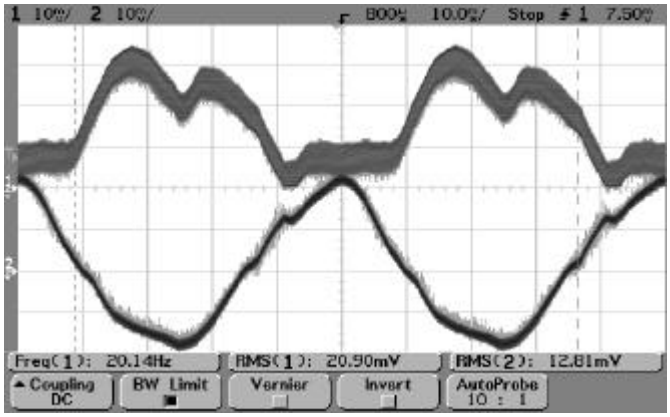

Fig. 13: No-load experimental phase currents. 2A/div. Top trace: Ch. 1, Phase *b*. Bottom trace: Ch. 2, Neutral current.

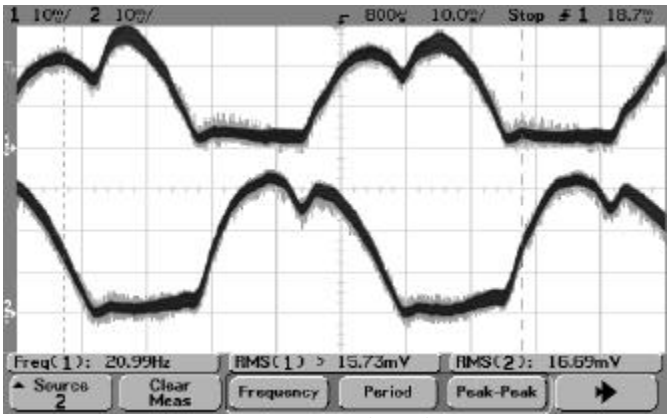

Fig. 14: Experimental phase currents for half-rated torque operation. 2A/div. Top trace: Ch. 1, Phase *a*. Bottom trace: Ch. 2, Phase *c*.

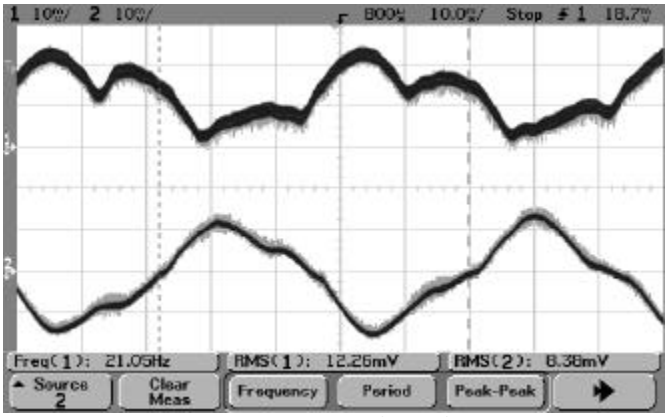

Fig. 15: Experimental phase currents for half-rated torque operation. 5A/div. Top trace: Ch. 1, Phase *b*. Bottom trace: Ch. 2, Neutral current.

The three phase currents in Figs. 12–13 show evidence that this is an open loop control technique as the phase *a* and *b* currents show contain some asymmetry. As expected by the series/parallel connected windings, the phase *b* currents contain a ripple component which is twice as large as phases *a* and *c*. Furthermore, the neutral current is a sinusoidal quantity as expected

Figures 14–15 show the measured phase and neutral currents for a commanded speed of 1200rpm with an applied load of ½rated torque. For this machine, this corresponds to a load of 0.7Nm. Like the unloaded case, the phase currents show the characteristic wave shape that is controlled by this algorithm with some asymmetry due to the non-ideal windings of the machine and open loop nature of the algorithm

In both the unloaded and loaded cases shown in Figs. 12–15, the currents show evidence of a third harmonic component which is larger than what is needed to achieve the desired waveshape. It is the belief of the authors that the non-ideal windings contain a third harmonic component that produces a rotating flux component with three times the number of poles of the fundamental component. This behavior is clearly not modeled in the zero sequence equivalent circuit shown in Fig. 5(b). For the machine tested, no information about the winding distribution of the stator was available to calculate what this affect would be, however, the experimental data indicates that the conventional zero sequence equivalent circuit may be incomplete, especially for smaller machines which inherently have fewer numbers of stator slots. This aspect of the research is under further investigation.

V. Conclusions

This paper proposes a new model based current shaping control for a three switch unipolar inverter for an induction machine. The new control method, based on the steady state equivalent circuit, is significant, as it requires zero current sensors, while previous control methods for this topology required three current sensors. Simulation results were presented to verify the feasibility of the proposed control algorithm. In addition, prototype hardware results indicate that this open loop control method can be used to control the speed and torque of induction machine with a unipolar drive topology.

The hardware results presented in this paper relied on artificially increasing the zero sequence reactance of the machine by adding an external inductance in the machine neutral path. As a result, additional research needs to be done

to gain a better understanding of how zero sequence currents influence the fundamental torque production of the machine before this method is commercially viable. However, since this method only relies on commissioned motor parameters, it remains an attractive topology/control candidate for integrated motor drive products where variable speed is desirable, but the high cost of a standard three-phase motor drive is prohibitive.

APPENDIX: MACHINE PARAMETERS

The 115/230V, 3-phase, 1 hp, 2 pole, induction machine with a squirrel cage rotor and dual wound stator used for this paper had the following characteristics when configured for high voltage operation.

$R_1 \approx 2.0\ \Omega$	$R_2 \approx 1.4\ \Omega$	$R_m \approx 465\ \Omega$
$L_1 \approx L_2 \approx 5.6\text{mH}$	$L_m \approx 218\ \text{mH}$	$f_{rated} = 87\ \text{Hz}$

ACKNOWLEDGEMENT

This work was supported primarily by the Center for Power Electronics Systems. CPES is a National Science Foundation ERC under Award Number EEC-9731677. The authors would also like to thank the Motorola Corporation for donating the DSP control board hardware and software used for the experimental results presented in this paper.

REFERENCES

[1] K. Phillips, “Power Electronics: Will Our Current Technical Vision Take Us to the Next Level of AC Drive Product Performance?,” *Conf. Rec. 35th IEEE IAS Annual Meeting*, Rome, Italy, 2000, vol. 1, pp. P1–P9.

[2] J. F. Eastham, A. R. Daniels, and R. T. Lipczynski, “A Novel Power Inverter Configuration,” *Conf. Rec. IEEE IAS Annual Meeting*, 1980, vol. 2, pp. 748-751.

[3] Heinz W. Van Der Broeck, J.D. Van Wyk, "A Comparative Investigation of a Three-Phase Induction Machine Drive with a Component Minimized Voltage-Fed Inverter Under Different Control Options," *IEEE Trans. on Ind. Applic.*, Vol. IA-20, No. 2, March/April 1984, pp. 309-320.

[4] P. D. Evans, R. C. Dodson, and J. F. Eastham, “Delta Inverter,” *Proc. IEE*, vol. 127, Pt. B, November 1980, pp. 333-340.

[5] B. A. Welchko, and T. A. Lipo, “A Novel Variable Frequency Three-Phase Induction Motor Drive System Using Only Three Controlled Switches,” *Conf. Rec. 35th IEEE IAS Annual Meeting*, Rome, Italy, 2000, vol. 3, pp. 1468–1473.

[6] K. Koga, R. Ueda, and T. Sonoda, “Constitution of V/f Control for Reducing the Steady State Speed Error to Zero in Induction Motor Drive System,” *Conf. Rec. IEEE IAS Annual Meeting*, 1990, vol. 1, pp. 639–646.

[7] A. Muñoz-García, T. A. Lipo, and D. W. Novotony, “A New Induction Motor Open-Loop Speed Control Capable of Low Frequency Operation,” *Conf. Rec. 32nd IEEE IAS Annual Meeting*, New Orleans, LA, 1997, vol. 1, pp. 579-586.

[8] D. W. Novotony, and T. A. Lipo, *Vector Control and Dynamics of AC Drives*, Oxford University Press, 1996.